Olfactory receptor-based CNT-FET sensor for the detection of DMMP as a simulant of sarin

Jin Yoo, Daesan Kim, Heehong Yang, Minju Lee, So-Ong Kim, Hwi Jin Ko, Seunghun Hong, Tai Hyun Park

Olfactory receptor-based CNT-FET sensor for the detection of DMMP as a simulant of sarin

Jin Yoo[a, †], Daesan Kim [b, †], Heehong Yang[a], Minju Lee[c], So-ong Kim[a], Hwi Jin Ko[a], Seunghun Hong[c*] and Tai Hyun Park[a]**

[a]School of Chemical and Biological Engineering, Institute of Chemical Processes, Seoul National University, Seoul 08826, Republic of Korea.

[b]Department of Biophysics and Chemical Biology, Seoul National University, Seoul 08826, Republic of Korea.

[c]Department of Physics and Astronomy and Institute of Applied Physics, Seoul National University, Seoul 08826, Republic of Korea.

[†]These authors contributed equally to this work.

* Corresponding author at: Department of Physics and Astronomy and Institute of Applied Physics, Seoul National University, Seoul 08826, Republic of Korea.

**Corresponding author at: School of Chemical and Biological Engineering, Seoul National University, Seoul 08826, Republic of Korea.

Tel: +82-2-880-8020; Fax: +82-2-875-9348;

E-mail: shong@phya.snu.ac.kr (S. Hong), thpark@snu.ac.kr (T. H. Park)

Abstract

Dimetyl metylphosphonate (DMMP) is a simulant of sarin, which is a representative of nerve agents. Sarin is an organophosphorus toxic compound that is an inhibitor of acetylcholinesterase, paralyzing human neurotransmission and the autonomic nervous system. Detection of these nerve agents has been considered important for safety issues to prevent terrorism and to counter military threats. Although there have been various studies on sensors for detecting DMMP as a simulant of sarin, limitations still exist in specificity, sensitivity, and reliability. To overcome these limitations, we utilized a human olfactory receptor (hOR)-based single-walled carbon nanotube-field effect transistor (swCNT-FET) as a platform for the detection of DMMP. The hORs have high specificity for their certain target molecules. swCNT-FET can also convert biological signals of hORs to electrical signals with high sensitivity. By screening of hORs, hOR2T7 with high selectivity for DMMP was selected, and it was produced for development of the hOR2T7-conjugated bioelectronic nose (hOR2T7 B-nose). A hOR2T7 B-nose was able to selectively detect DMMP at a concentration of 10 fM. This shows ultrasensitive and selective performance for the detection of DMMP as a tool for sensing chemical warfare agents (CWAs), which could be used for practical applications in the field of safety.

Keywords: DMMP, CWAs, olfactory receptor, swCNT-FET, bioelectronic nose, terrorism

1. Introduction

Dimethyl methylphosphonate (DMMP) is a structural simulant of sarin, a chemical warfare agent (CWA) [1, 2]. CWAs are those used in chemical weapons, such as sarin, soman, and cyanide. Among CWAs, sarin and soman are representatives of nerve agents [3]. Sarin gas is an organophosphorous toxin that inactivates acetylcholinesterase in the human body, making the control of neurotransmitters difficult at the cholinergic synapses, and paralyzing neurons in the body, leading to death [4]. Previous studies show that when exposed to or inhaling 10 mg/m^3 of sarin vapor for 10 min, approximately half of the exposed people died [5].

In recent years, there have been various studies on the detection of CWAs, especially of DMMP as the simulant of sarin. Methods for the sensitive and practical sensing of DMMP, such as chemical sensors [6-9], colorimetric analysis [10, 11], and the microcantilever (MCL) [12], have been introduced. However, several challenges still remain, such as selectivity, sensitivity, sensing condition, and complex sensing procedures.

There have been many studies on the bioelectronic nose and bioelectronic tongue [13-15] using human olfactory and taste receptors for the sense of a variety of molecules that have to be detected in everyday life. In particular, most studies focus on the bioelectronic nose, because the number of molecules that can be detected is enormous, and it therefore can be applied to various fields. Many researchers have reported a bioelectronic nose using human olfactory receptors (hORs) as a tool for the selective and sensitive detection of target molecule [14, 16, 17]. The hORs expressed in the human olfactory epithelium have the ability to sensitively detect specific target molecules in various substances. The hORs can be combined with nanomaterials, such as graphene [18], carbon nanotubes (CNTs) [19], conducting polymer, and polypyrole (PPy)-nanotube [20], to enhance sensitivity through the conversion of biological

signals to electrical current changes [13, 14]. Especially, CNTs have a large surface area to volume ratio due to their unique one-dimensional nanoscale structures. Thus, the electrical properties of CNTs could be effectively changed by the binding of odorants to hORs immobilized on the CNT surface. [21]

Although these hOR-conjugated bioelectronic noses (hOR B-noses) have high performance in sensitivity and selectivity, there are still some issues in the stability, reusability, or productivity of biomaterials [22, 23]. It has also been reported that the purified and reconstituted proteins potentially have high stability, and can be overproduced from *Escherichia coli* (*E. coli*). This bacterial expression system can have many advantages, such as fast and massive production, and simplicity. A protein-based B-nose can offer great advantage in high productivity and specific detection. [24, 25]

Herein, we report a hOR protein-based single-walled CNT field-effect transistor (swCNT-FET) for the selective and sensitive detection of DMMP. It can be used to detect DMMP in real time under normal conditions. This work is expected to provide a practical and easy-to-use sensor for CWAs, such as sarin.

2. Materials and Methods

2.1 Mammalian cell culture and expression of olfactory receptors (ORs)

The cells used in the experiment were Hana3A cells. Hana3A cells are derived from human embryonic kidney 293T (HEK-293T) cells, which stably expresses RTP1L, RTP2, REEP1, and $G_{\alpha olf}$ proteins to confirm the function of the olfactory receptor [26, 27]. The cells were cultured at 37 °C and 5 % CO_2 in MEM medium containing 10 % fetal bovine serum (FBS) at a concentration of 100 μg/mL penicillin streptomycin (Sigma-Aldrich, USA), 1.25 μg/mL amphotericin B (Sigma-Aldrich, USA), and 1 μg/mL of puromycin (Sigma-Aldrich, USA). Olfactory receptors were expressed by transfection of a plasmid in which olfactory receptor gene was inserted using Lipofectamine 3000 (Invitrogen, USA). Olfactory receptor genes were subcloned into pcDNA3 mammalian expression vectors (Invitrogen, USA) containing human rhodopsin (Rho tag) for expression confirmation [28]. Hana3A cells were plated in 96-well plates with 1×10^4 cells/well for 24 h. After this, Hana3A cells were transfected with 10 ng/well of pCRE-Luc, 5 ng/well of OR, 5 ng/well of pSV40-RL, 5 ng/well of RTP1s, and 2.5 ng/well of M3R, and incubated for (18–24) h [29, 30]. Expression of OR on cell surface was confirmed by western blot analysis. Later, at 24 h after transfection, the cells were washed with PBS and protein inhibition cocktail. The cells were lysed by sonication (2 s on/off, 5 min). The supernatant was obtained by centrifugation at 15,000× g for 30 min. After boiling, sample proteins were loaded onto SDS-page gels, and transferred to PVDF membrane (Bio-Rad, USA). The membrane was blocked by TBS with 0.1 % tween-20 (TBST) and 5 % skim milk. The primary antibody used in this report was DYKDDDDK rabbit monoclonal antibody (Cell Signaling Technology, USA), which was treated to the membrane overnight at a 1:1,000 dilution in TBST with 1 % skim milk at 4 °C. The membrane was washed with TBST for 20

min, and treated with secondary antibody. Goat anti-rabbit IgG-HRP was used as secondary antibody (Santa Cruz, USA) which was treated to the membrane for 1 h at a 1:500 dilution in TBST with 5 % skim milk at 4 °C. The substrate was Lumina Forte Western HRP substrate. (Merck Millipore, Germany)

2.2 Biological screening of olfactory receptors repertoire

The Dual-Glo Luciferase Assay System (Promega, USA) was used to find which receptor responds to target molecules. Transfection medium was replaced with diluted 1 mM odorants in CD293 (Gibco, USA) with L-glutamate 24 h after transfection. At 4 h after odorant treatment, luminescence was measured with Spark™ 10M multimode microplate reader (Tecan, Switzerland). The measured luminescence was normalized to luciferase activity by normalization formula [CRE/Renilla (odorant) – CRE/Renilla (negative control)] / [CRE/Renilla (positive control) – CRE/Renilla (negative control)]. Negative control was obtained by treating only DMSO (dimethyl sulfoxide, Sigma-Aldrich, USA), while positive control was obtained by treating 1 μM forskolin (Sigma-Aldrich, USA) [31]. For odorant stimulation, each odorant was diluted in DMSO. We prepared odorants, such as dimethyl methylphosphonate (DMMP, Sigma-Aldrich, USA), dimethyl phosphite (DMP, Sigma-Aldrich, USA), diethyl phosphite (DEP, Sigma-Aldrich, USA), diethyl ethylphosphonate (DEEP, Sigma-Aldrich, USA), diethyl allyl phosphate (DEAP, Sigma-Aldrich, USA), trimethyl phosphate (TMP, Sigma-Aldrich, USA), linalool (Fluka, USA), Nerol (Fluka, USA), amyl butyrate (Sigma-Aldrich, USA), ethyl butyrate (Sigma-Aldrich, USA), and guaiacol (Sigma-Aldrich, USA) for hOR activity analysis.

2.3 hOR protein production, purification, and reconstitution

As in previous studies, GPCRs including hORs were overexpressed in *E. coli* with bacterial expression vectors [32, 33]. The pET-DEST42 vector contained hOR genes, and transformed to BL21 *E. coli* cells. The cells were incubated with LB media containing ampicillin. When OD reached 0.5, the cells were treated with IPTG (Sigma-Aldrich, USA), and were incubated for 4 h at 37 °C. The the cells were then lysed by sonication with 5 s on/off for 10 min for 2 times. Insoluble pellet after centrifugation (15,000× *g*, 4 °C, 20 min) was solubilized in 75 mL of 0.1 M tris-HCl (pH 8.0), 20 mM sodium dodecyl sulfate (SDS), 100 mM dithiothreitol (DTT), and 1 mM EDTA at 30 °C, and incubated in 120 rpm shaking incubator overnight. After solubilization, dialysis was executed by a 10K MWCO dialysis cassette (Thermo Scientific, USA) with 0.1 M sodium phosphate (pH 8.0) and 10 mM SDS. After filtering of the protein using 0.2 μm bottle top filter (Thermo Scientific, USA), the protein was passed through 5 mL HisTrap HP column (GE Healthcare, USA), and eluted from the column in the buffer at 0.1 M sodium phosphate (pH 6.0) and 10 mM SDS. The purified protein that has denatured form was refolded into detergent micelles, which were used to refold the structure of GPCR [34-36].

2.4 Fabrication of swCNT-FET

Prevalent photolithography and metal deposition were utilized to develop a swCNT-FET device. First, photoresist (PR, Az5214) was patterned on the SiO_2 wafer to make swCNT patterned channels. Then, the PR patterned wafer was immersed in octadecyltrichlorosilane (OTS) solution (OTS:Hexane = 1:400) for 7 min. Here, OTS molecules were adsorbed onto the bare surface of the patterned wafer, to form a self-assembled monolayer (SAM). To remove the PR regions, the OTS patterned wafer was rinsed by acetone and ethanol. The wafer was

incubated in swCNT solution (0.05 mg/mL in dichlorobenzene) for 20 s. In this process, swCNTs were specifically adsorbed on the exposed SiO_2 surface, due to the hydrophobicity of OTS. After the fabrication of swCNT channels, drain and source electrodes (Ti/Au, 10/30 nm) were assembled *via* thermal evaporation method. Lastly, to keep any solution off, drain and source electrodes were passivated by PR (DNR).

2.5 Development of a bioelectronic nose for the detection of DMMP

A CNT-FET channel region was treated with 2 L of methanol containing 0.1 M PSE, and incubated at room temperature (RT) for 1 h. Then, the patterned wafer was rinsed with DDW to remove unbound PSE; and the same region was treated with 2 μL of hOR2T7 protein at RT for 1 h. During the immobilization process, a moist environment was maintained, to prevent drying. hOR2T7 was immobilized on the CNT channel *via* the linker molecules, PSE. To monitor the electrical signal of the bioelectronic nose, a buffer zone of 20 μL was formed on the channel region, using detergent micelle refolding buffer. The DMMP samples were diluted with PBS, and 10 μL of the diluted sample was added onto the channel of the bioelectronic nose. The dilution range was from 10^{-16} to 10^{-7}. Conductance changes between the source and drain electrodes were monitored using a Keithley 2636A source meter (Keithley, USA), and a MST 8000 probe station (MS Tech, South Korea).

3. Results and Discussion

3.1 Screening hORs using cell-based analysis

Prior to screening ORs, a cytotoxicity assay was performed to confirm the toxicity of DMMP to Hana3A cells. **Fig. S1** of the Supporting Information (SI) shows that the DMMP does not influence the viability of Hana3A cells in the range of concentration of (30 μM to 10 mM). The result indicates that there is no interference by DMMP in the biological activity assay of Hana3A cells. Based on this result, the screening of hORs was performed at the concentration of 1 mM DMMP using the luciferase assay known as a high-throughput ORs screening method [27]. **Fig. S2** of SI shows the western blot analysis of hORs expressed in Hana3A cell, showing that the hORs were successfully expressed in the Hana3A cell. We tested 120 hORs. **Fig. 2a** shows that among the 120 hORs, seven hORs indicated by *'s (hOR10A4, hOR5M10, hOR2D2, hOR2T7, hOR8U1, hOR8G5, and hOR2AG2) bind to DMMP, while only four hORs (hOR5M10, hOR2T7, hOR8G5, and hOR2AG2) strongly bind to DMMP. The relative responses of hORs were compared using a normalization formula as defined in the Materials and Methods. **Fig. 2b** shows the dose-dependent response of the four hORs. In the range of concentrations of (100 μM to 10 mM), the responses of the four hORs increased in a dose-dependent manner. In order to select the hOR that selectively responds to DMMP, selectivity test was conducted with two types of odor molecule groups using luciferase assay (**Fig. 2c and d**). One group is odor molecules that have a chemical structure similar to DMMP. The other group is odor molecules that have a smell similar to DMMP. We added to the second group one more molecule of smoky smell, which might exist in warfare situations. Odor molecules that are structurally similar to DMMP are dimethyl phosphite (DMP), diehtyl phosphite (DEP), diethyl ethylphosphonate (DEEP), diethyl allyl phosphate (DEAP), and trimethyl phosphate

(TMP). **Fig. S3** shows the structure of those odor molecules. Odor molecules with similar smell to DMMP are linalool, nerol, amyl butyrate, and ethyl butyrate, which are generally recognized by human as pleasant smells. Guaiacol is a molecule known to have a smoky odor. In the selectivity test, **Fig. 2c** shows that among the four hORs, only hOR2T7 selectively binds to DMMP, while hOR8G5 binds to all the five odor molecules, DMMP, DMP, DEP, DEEP, and DEAP, indicating that hOR8G5 is broadly tuned to structurally similar odor molecules. **Fig. 2d** is a result of the selectivity test with the molecules that have similar odor to DMMP. The result shows that hOR2T7 and hOR8G5 can discriminate DMMP from other molecules with similar smell. None of the four ORs bound with a smoky odor molecule. The results in **Fig. 2** demonstrate that hOR2T7 can be applied to B-nose for the selective detection of DMMP, which is a simulant of sarin.

3.2 Production of hOR2T7 in E. coli

The hOR2T7 was produced from *E. coli,* purified with column chromatography, and reconstituted into detergent micelles for the development of protein-based biosensor. **Fig. 3a** shows the SDS-PAGE and western blot analysis of the hOR2T7. The yield of hOR2T7 was 0.2 ~ 0.5 mg per liter culture after finishing the purification step. Since the protein is denatured during the purification process, it should be reconstituted with a hydrophobic environment. Thus to recover its natural form, the purified hOR2T7 was reconstituted into detergent micelles. After the reconstitution of hOR2T7, tryptophan fluorescence quenching analysis was carried out to investigate the binding property of hOR2T7. **Fig. 3b** shows that as the DMMP concentration increased from (1 to 20) μM, the fluorescence of hOR2T7 was quenched gradually. When the tryptophan residues of the protein were excited at a wavelength of 280

nm, the emission was observed at a wavelength range of (340 to 350) nm [23, 37]. From the analysis of amino acids, it was confirmed that hOR2T7 has three tryptophan residues. Thus, when DMMP was bound to hOR2T7, the conformational change of hOR2T7 hides the tryptophan residues, resulting in the inhibition of their excitation; and then the fluorescence intensity of hOR2T7 was quenched. This quenching clearly demonstrates that the reconstituted hOR2T7 restored its normal function.

3.3 Characteristics of hOR2T7 B-nose

Fig. 3c and d show the characteristics of hOR2T7 B-nose. **Fig. 3c** shows the atomic force microscopy (AFM) images and height profile graph to confirm the immobilization of hOR2T7 on the CNT channel. They were imaged *via* tapping mode AFM with scan rates of (0.4 and 0.1) Hz. The left and right AFM images show the swCNT surfaces before and after the immobilization of the receptor onto CNT surfaces, respectively. The height profile graph compares the height profiles at the same region of the AFM images. The black and red lines in the profile graph indicate the height of swCNTs before and after the immobilization of hOR2T7 on the CNT channel, respectively. The peaks of the red line are higher than those of the black one by (3 – 4) nm. This indicates that the hOR2T7 was successfully immobilized on the CNT channel. We also compared the *I–V* characteristics of a CNT sensor before and after the immobilization of hOR2T7 on the CNT channel, to confirm that the function of CNT sensor remains intact, even after the protein immobilization process. **Fig. S4** of SI shows the *I–V* characteristics of the sensor before and after the immobilization, which indicate that the electrical properties of the sensor were well maintained. In addition, **Fig. 3d** shows that the

electrical current decreased by the immobilization of hOR2T7 on the CNT surface, maintaining the p-type semiconductor characteristics of the sensor.

3.4 Real-time detection of DMMP using the hOR2T7 B-nose

The real-time responses of hOR2T7 B-nose to DMMP were confirmed by measuring the drain-source conductance changes, after the injection of DMMP solution containing serial concentrations of DMMP. The sensing methods were similar to those in previous studies, [38-40] in which the binding between hOR and the ligand causes a conformational change in the hOR, and change in conductance of the CNT channels [41, 42]. In the mechanism of olfactory transduction in the olfactory epithelium involves OR switching from a conformationally inactive state towards an active state upon ligand binding [43]. Thus, a conformational change of olfactory receptor by the interaction between olfactory receptors and target odor molecules, affects a field effect on the sensing channels, and derives a change of conductance between source and drain electrodes [44]. **Fig. 4a** shows the real-time responses of a hOR2T7 B-nose to DMMP in the range of concentrations of (10 fM to 100 nM). The electrical conductance of the hOR2T7 B-nose exhibited a sharp increase after the injection of DMMP. The responses were saturated at a concentration of 10 nM. These results show that a hOR2T7 B-nose can detect DMMP down to fM level with higher sensitivity than any other DMMP sensor developed so far. **Fig. 4b** is the normalized sensitivity curve of hOR2T7 B-nose to DMMP in the range of concentrations of (10 fM to 0.1 μM), and shows the dose-dependent responses of hOR2T7 B-nose to DMMP. **Fig. S5** shows the real-time current changes with various DMMP concentrations. Also, selectivity tests were performed to confirm that the selectivity of hOR2T7 B-nose is the same as the experimental result of the cellular level through the real-time analysis

of hOR2T7 B-nose. **Fig. 4c** is the result of the selectivity test of hOR2T7 B-nose to structurally similar odor molecules, which are DMP, DEP, DEAP, and DEEP, and shows that the hOR2T7 B-nose has a specificity with DMMP, which is the same as the result of the cellular assay. **Fig. 4d** shows the selectivity test of hOR2T7 B-nose to various molecules with similar odor to DMMP, or with a smoky odor. Amyl butyrate, ethyl butyrate, linalool, and nerol are molecules with similar odor, while guaiacol is a molecule with smoky odor. This result shows that hOR2T7 B-nose also has a selectivity only to DMMP, among various odor molecules with pleasant and smoky smells. Each analysis was carried out with the same hOR2T7 B-nose in real-time, and odorant molecules were added in order. These results clearly show that the binding property of hOR2T7 observed in the cellular analysis was successfully reproduced in B-nose using hOR2T7, which was produced in *E. coli*, purified, and reconstituted. The micelle-based bioelectronic nose was stable at least for three weeks [45].

4. Conclusions

hOR2T7 B-nose was fabricated by the conjugation of a reconstituted hOR2T7 with swCNT-FET platform. The hOR2T7 B-nose detected its target molecule, DMMP, which is a nerve agent simulant, with high sensitivity and selectivity. hOR2T7B-nose detected DMMP at the concentration of 10 fM, and discriminated the target molecule from an odor molecule with smoky smell, as well as odor molecules with similar structure and similar pleasant smell. These results indicate that hOR2T7 B-nose could effectively and selectively detect a nerve agent simulant with high sensitivity. However, it is also still possible that hOR2T7 will not bind to sarin itself, because hOR2T7 is so specific to DMMP. In this case, we can consider hOR8G5 as an alternative. Interestingly, hOR8G5 broadly responded to odor molecules with a similar structure to DMMP, but did not respond to guaiacol or odor molecules with a similar smell to DMMP. Many studies on olfactory receptors have also reported that the hORs could broadly detect molecules that have structural similarity [46, 47]. This suggests that if hOR2T7 is not working for the detection of sarin, hOR8G5 can be used as an alternative choice for the detection of sarin, an actual target molecule. This B-nose technology can be used for early response to nerve gas attacks in various situations, including terrorism and military threats.

Acknowledgements

This work was supported by the National Research Foundation of Korea (NRF), funded by the Ministry of Science and ICT (MSIT) of Korea (grant agreement No. 2018R1A2B3004498), and the European Research Council (ERC), under the European Union's Horizon 2020 research and innovation programme (grant agreement No. 682286).

References

[1] J. Novak, E. Snow, E. Houser, D. Park, J. Stepnowski, R. McGill, Nerve agent detection using networks of single-walled carbon nanotubes, Applied physics letters, 83(2003) 4026-8.

[2] R. Yoo, S. Yoo, D. Lee, J. Kim, S. Cho, W. Lee, Highly selective detection of dimethyl methylphosphonate (DMMP) using CuO nanoparticles/ZnO flowers heterojunction, Sensors and Actuators B: Chemical, 240(2017) 1099-105.

[3] L.K. Wright, R.B. Lee, N.M. Vincelli, C.E. Whalley, L.A. Lumley, Comparison of the lethal effects of chemical warfare nerve agents across multiple ages, Toxicology letters, 241(2016) 167-74.

[4] J. Bajgar, Organophosphates / nerve agent poisoning: mechanism of action, diagnosis, prophylaxis, and treatment, Advances in clinical chemistry, 38(2004) 151-216.

[5] M.A. Brown, K.A. Brix, Review of health consequences from high-, intermediate-and low-level exposure to organophosphorus nerve agents, Journal of Applied Toxicology, 18(1998) 393-408.

[6] O.S. Kwon, C.S. Park, S.J. Park, S. Noh, S. Kim, H.J. Kong, et al., Carboxylic acid-functionalized conducting-polymer nanotubes as highly sensitive nerve-agent chemiresistors, Scientific reports, 6(2016).

[7] M. Šťastný, J. Tolasz, V. Štengl, J. Henych, D. Žižka, Graphene oxide/MnO 2 nanocomposite as destructive adsorbent of nerve-agent simulants in aqueous media, Applied Surface Science, 412(2017) 19-28.

[8] A.A. Tomchenko, G.P. Harmer, B.T. Marquis, Detection of chemical warfare agents using nanostructured metal oxide sensors, Sensors and Actuators B: Chemical, 108(2005) 41-55.

[9] F. Wang, H. Gu, T.M. Swager, Carbon nanotube/polythiophene chemiresistive sensors for chemical warfare agents, Journal of the American Chemical Society, 130(2008) 5392-3.

[10] P.M. Reddy, S.-R. Hsieh, C.-J. Chang, J.-Y. Kang, Detection of cyanide ions in aqueous solutions using cost effective colorimetric sensor, Journal of Hazardous Materials, 334(2017) 93-103.

[11] Y. Zhou, J.F. Zhang, J. Yoon, Fluorescence and colorimetric chemosensors for fluoride-ion detection, Chemical reviews, 114(2014) 5511-71.

[12] N.-J. Choi, Y.-S. Lee, J.-H. Kwak, J.-S. Park, K.-B. Park, K.-S. Shin, et al., Chemical warfare agent sensor using MEMS structure and thick film fabrication method, Sensors and Actuators B: Chemical, 108(2005) 177-83.

[13] T.H. Kim, B.Y. Lee, J. Jaworski, K. Yokoyama, W.-J. Chung, E. Wang, et al., Selective and sensitive TNT sensors using biomimetic polydiacetylene-coated CNT-FETs, ACS nano, 5(2011) 2824-30.

[14] J.H. Lim, J. Park, E.H. Oh, H.J. Ko, S. Hong, T.H. Park, Nanovesicle-Based Bioelectronic Nose for the Diagnosis of Lung Cancer from Human Blood, Advanced healthcare materials, 3(2014) 360-6.

[15] H.S. Song, O.S. Kwon, S.H. Lee, S.J. Park, U.-K. Kim, J. Jang, et al., Human taste receptor-functionalized field effect transistor as a human-like nanobioelectronic tongue, Nano letters, 13(2013) 172-8.

[16] S.H. Lee, H.J. Jin, H.S. Song, S. Hong, T.H. Park, Bioelectronic nose with high sensitivity and selectivity using chemically functionalized carbon nanotube combined with human olfactory receptor, Journal of biotechnology, 157(2012) 467-72.
[17] S.W. Cho, T.H. Park, Comparative Evaluation of Sensitivity to Hexanal Between Human and Canine Olfactory Receptors, Biotechnology and Bioprocess Engineering, 24(2019) 1007-12.
[18] S.J. Park, O.S. Kwon, S.H. Lee, H.S. Song, T.H. Park, J. Jang, Ultrasensitive flexible graphene based field-effect transistor (FET)-type bioelectronic nose, Nano letters, 12(2012) 5082-90.
[19] J. Park, J.H. Lim, H.J. Jin, S. Namgung, S.H. Lee, T.H. Park, et al., A bioelectronic sensor based on canine olfactory nanovesicle–carbon nanotube hybrid structures for the fast assessment of food quality, Analyst, 137(2012) 3249-54.
[20] H. Yoon, S.H. Lee, O.S. Kwon, H.S. Song, E.H. Oh, T.H. Park, et al., Polypyrrole nanotubes conjugated with human olfactory receptors: high-performance transducers for FET-type bioelectronic noses, Angewandte Chemie International Edition, 48(2009) 2755-8.
[21] B.L. Allen, P.D. Kichambare, A. Star, Carbon nanotube field-effect-transistor-based biosensors, Advanced Materials, 19(2007) 1439-51.
[22] H. Yang, H.S. Song, S.R. Ahn, T.H. Park, Purification and functional reconstitution of human olfactory receptor expressed in Escherichia coli, Biotechnology and bioprocess engineering, 20(2015) 423-30.
[23] L. Kaiser, J. Graveland-Bikker, D. Steuerwald, M. Vanberghem, K. Herlihy, S. Zhang, Efficient cell-free production of olfactory receptors: detergent optimization, structure, and ligand binding analyses, Proceedings of the National Academy of Sciences, 105(2008) 15726-31.
[24] S.J. Park, H. Yang, S.H. Lee, H.S. Song, C.S. Park, J. Bae, et al., Dopamine Receptor D1 Agonism and Antagonism Using a Field-Effect Transistor Assay, ACS nano, (2017).
[25] M. Son, D. Kim, K.S. Park, S. Hong, T.H. Park, Detection of aquaporin-4 antibody using aquaporin-4 extracellular loop-based carbon nanotube biosensor for the diagnosis of neuromyelitis optica, Biosensors and Bioelectronics, 78(2016) 87-91.
[26] L. Wu, Y. Pan, G.-Q. Chen, H. Matsunami, H. Zhuang, Receptor-transporting protein 1 short (RTP1S) mediates translocation and activation of odorant receptors by acting through multiple steps, Journal of Biological Chemistry, 287(2012) 22287-94.
[27] H. Zhuang, H. Matsunami, Evaluating cell-surface expression and measuring activation of mammalian odorant receptors in heterologous cells, Nature protocols, 3(2008) 1402.
[28] H. Zhuang, H. Matsunami, Synergism of accessory factors in functional expression of mammalian odorant receptors, Journal of Biological Chemistry, 282(2007) 15284-93.
[29] Y.R. Li, H. Matsunami, Activation state of the M3 muscarinic acetylcholine receptor modulates mammalian odorant receptor signaling, Science signaling, 4(2011) ra1.
[30] J.D. Mainland, A. Keller, Y.R. Li, T. Zhou, C. Trimmer, L.L. Snyder, et al., The missense of smell: functional variability in the human odorant receptor repertoire, Nature neuroscience, 17(2014)

114-20.
[31] K.B. Seamon, W. Padgett, J.W. Daly, Forskolin: unique diterpene activator of adenylate cyclase in membranes and in intact cells, Proceedings of the National Academy of Sciences, 78(1981) 3363-7.
[32] O.S. Kwon, S.H. Lee, S.J. Park, J.H. An, H.S. Song, T. Kim, et al., Large-scale graphene micropattern nano-biohybrids: high-performance transducers for FET-type flexible fluidic HIV immunoassays, Advanced Materials, 25(2013) 4177-85.
[33] S.H. Lee, O.S. Kwon, H.S. Song, S.J. Park, J.H. Sung, J. Jang, et al., Mimicking the human smell sensing mechanism with an artificial nose platform, Biomaterials, 33(2012) 1722-9.
[34] G. Ishihara, M. Goto, M. Saeki, K. Ito, T. Hori, T. Kigawa, et al., Expression of G protein coupled receptors in a cell-free translational system using detergents and thioredoxin-fusion vectors, Protein expression and purification, 41(2005) 27-37.
[35] C. Klammt, D. Schwarz, K. Fendler, W. Haase, V. Dötsch, F. Bernhard, Evaluation of detergents for the soluble expression of α-helical and β-barrel-type integral membrane proteins by a preparative scale individual cell-free expression system, The FEBS journal, 272(2005) 6024-38.
[36] C. Klammt, D. Schwarz, F. Löhr, B. Schneider, V. Dötsch, F. Bernhard, Cell-free expression as an emerging technique for the large scale production of integral membrane protein, The FEBS journal, 273(2006) 4141-53.
[37] H. Kiefer, J. Krieger, J.D. Olszewski, G. Von Heijne, G.D. Prestwich, H. Breer, Expression of an olfactory receptor in Escherichia coli: purification, reconstitution, and ligand binding, Biochemistry, 35(1996) 16077-84.
[38] S.R. Ahn, J.H. An, H.S. Song, J.W. Park, S.H. Lee, J.H. Kim, et al., Duplex bioelectronic tongue for sensing umami and sweet tastes based on human taste receptor nanovesicles, ACS nano, 10(2016) 7287-96.
[39] S.J. Park, S.H. Lee, H. Yang, C.S. Park, C.-S. Lee, O.S. Kwon, et al., Human dopamine receptor-conjugated multidimensional conducting polymer nanofiber membrane for dopamine detection, ACS applied materials & interfaces, 8(2016) 28897-903.
[40] M. Son, D. Kim, J. Kang, J.H. Lim, S.H. Lee, H.J. Ko, et al., Bioelectronic Nose Using Odorant Binding Protein-Derived Peptide and Carbon Nanotube Field-Effect Transistor for the Assessment of Salmonella Contamination in Food, Analytical chemistry, 88(2016) 11283-7.
[41] J.H. Ahn, J.H. Lim, J. Park, E.H. Oh, M. Son, S. Hong, et al., Screening of target-specific olfactory receptor and development of olfactory biosensor for the assessment of fungal contamination in grain Screening of target-specific olfactory receptor and development of olfactory biosensor for the assessment of fungal contamination in grain, Sens Actuator B-Chem, 210(2015) 9-16.
[42] O.S. Kwon, H.S. Song, S.J. Park, S.H. Lee, J.H. An, J.W. Park, et al., An Ultrasensitive, Selective, Multiplexed Superbioelectronic Nose That Mimics the Human Sense of Smell, Nano Letters, 15(2015) 6559-67.

[43] A. Sharma, R. Kumar, I. Aier, R. Semwal, P. Tyagi, P. Varadwaj, Sense of smell: structural, functional, mechanistic advancements and challenges in human olfactory research, Current neuropharmacology, 17(2019) 891-911.
[44] M. Son, T.H. Park, The bioelectronic nose and tongue using olfactory and taste receptors: Analytical tools for food quality and safety assessment, Biotechnology advances, 36(2018) 371-9.
[45] J. Oh, H. Yang, G.E. Jeong, D. Moon, O.S. Kwon, S. Phyo, et al., Ultrasensitive, selective, and highly stable bioelectronic nose that detects the liquid and gaseous cadaverine, Analytical chemistry, 91(2019) 12181-90.
[46] L. Charlier, J. Topin, C. Ronin, S.-K. Kim, W.A. Goddard, R. Efremov, et al., How broadly tuned olfactory receptors equally recognize their agonists. Human OR1G1 as a test case, Cellular and molecular life sciences, 69(2012) 4205-13.
[47] J. Li, R. Haddad, S. Chen, V. Santos, C.W. Luetje, A broadly tuned mouse odorant receptor that detects nitrotoluenes, Journal of neurochemistry, 121(2012) 881-90.

Figure Captions

Fig. 1. Schematic representation of hOR-based CNT-FET sensor for the detection of DMMP.

Fig. 2. Screening of DMMP-binding hORs. (a) Response of 120 hORs to 1 mM DMMP. (b) Dose-dependent response curves of 4 hORs that strongly bind with DMMP. (c) Selectivity test of hOR5M10, hOR2T7, hOR8G5, and hOR2AG2 using DMMP and structurally similar molecules (DMP; dimethyl phosphite, DEP; diethyl phosphite, DEEP; diethyl ethylphosphite, DEAP; diethyl allyl phosphite). (d) Selectivity test of hOR5M10, hOR2T7, hOR8G5, and hOR2AG2 with DMMP, molecules with similar odor (linalool, nerol, amyl butyrate, ethyl butyrate) and a molecule with smoky odor (guaiacol). Error bar (standard of the mean), three replicates, $*P < 0.05$, $**P < 0.01$, $***P < 0.001$, in the two-way ANOVA model.

Fig. 3. Functional production of the hOR and fabrication of the bioelectronic nose by the immobilization of hOR on CNT-FET. (a) SDS-page and western blot analysis of the purified hOR2T7 protein. (b) Tryptophan fluorescence analysis of the reconstituted hOR2T7. (c) AFM images and height profile of bare CNT channel and CNT channel functionalized with hOR. (d) Gate profile of bare CNT channel and CNT channel functionalized with hOR.

Fig. 4. Detection of DMMP using a hOR2T7 B-nose. (a) Real-time responses of hOR2T7 B-nose to DMMP with various concentrations. (b) Dose-dependent response of hOR2T7 B-nose with DMMP. Error bar (standard of the mean), three replicates. (c) Real-time selectivity test of hOR2T7 B-nose with structurally similar molecules. (d) Real-time selectivity test of hOR2T7 B-nose with similar odor molecules and a smoky odor molecule.

Fig. 1

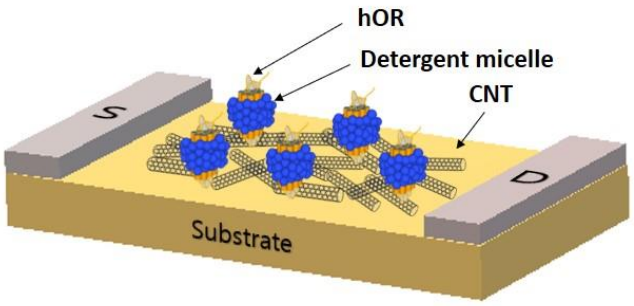

Fig. 2

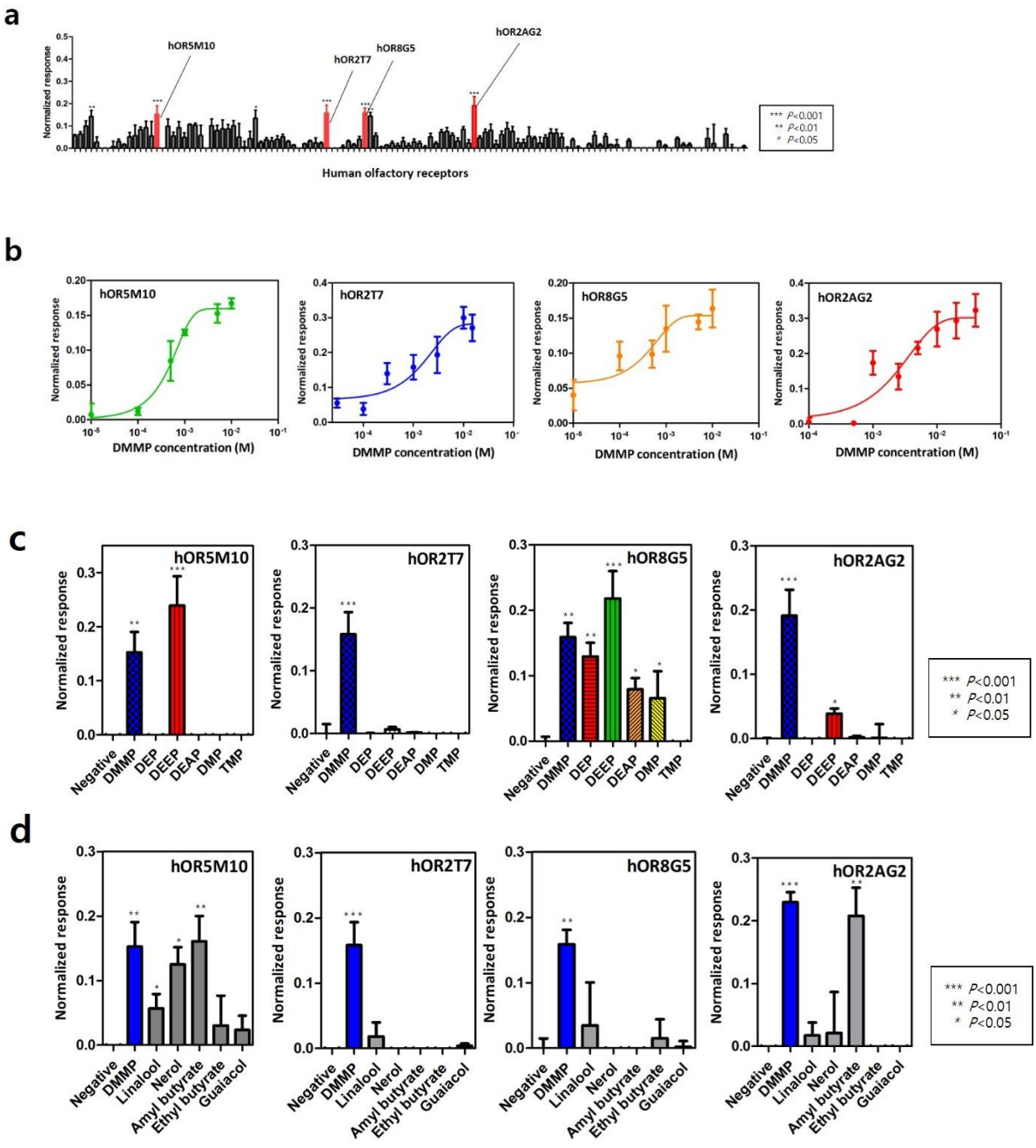
a
hOR5M10
hOR2T7
hOR8G5
hOR2AG2
Normalized response
Human olfactory receptors
*** P<0.001
** P<0.01
* P<0.05
b
hOR5M10
hOR2T7
hOR8G5
hOR2AG2
Normalized response
DMMP concentration (M)
c
hOR5M10
hOR2T7
hOR8G5
hOR2AG2
Normalized response
Negative
DMMP
DEP
DEEP
DEAP
DMP
TMP
*** P<0.001
** P<0.01
* P<0.05
d
hOR5M10
hOR2T7
hOR8G5
hOR2AG2
Normalized response
Negative
DMMP
Linalool
Nerol
Amyl butyrate
Ethyl butyrate
Guaiacol
*** P<0.001
** P<0.01
* P<0.05

Fig. 3

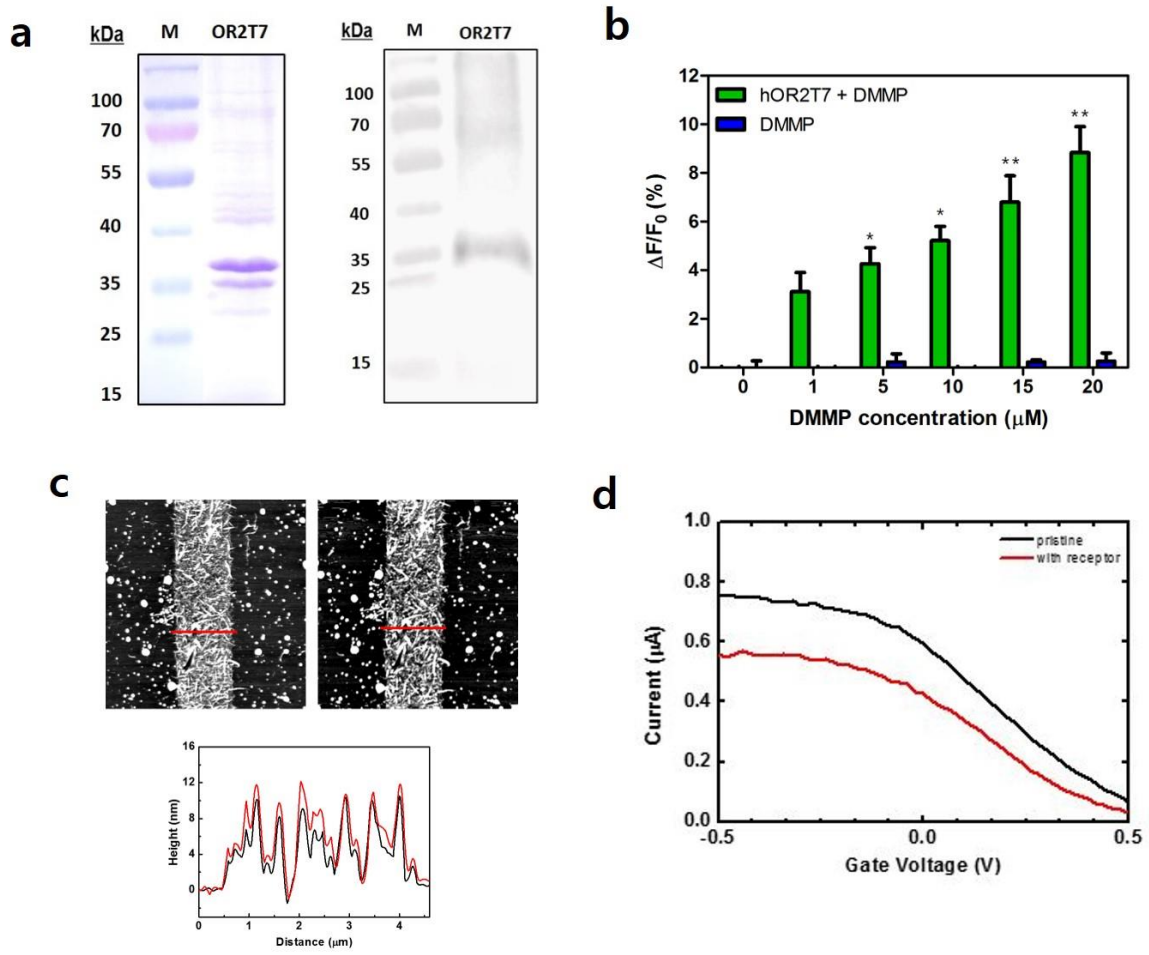
a
kDa
M
OR2T7
100
70
55
40
35
25
15
b
hOR2T7 + DMMP
DMMP
ΔF/F0 (%)
DMMP concentration (μM)
c
Height (nm)
Distance (μm)
d
pristine
with receptor
Current (μA)
Gate Voltage (V)

Fig. 4

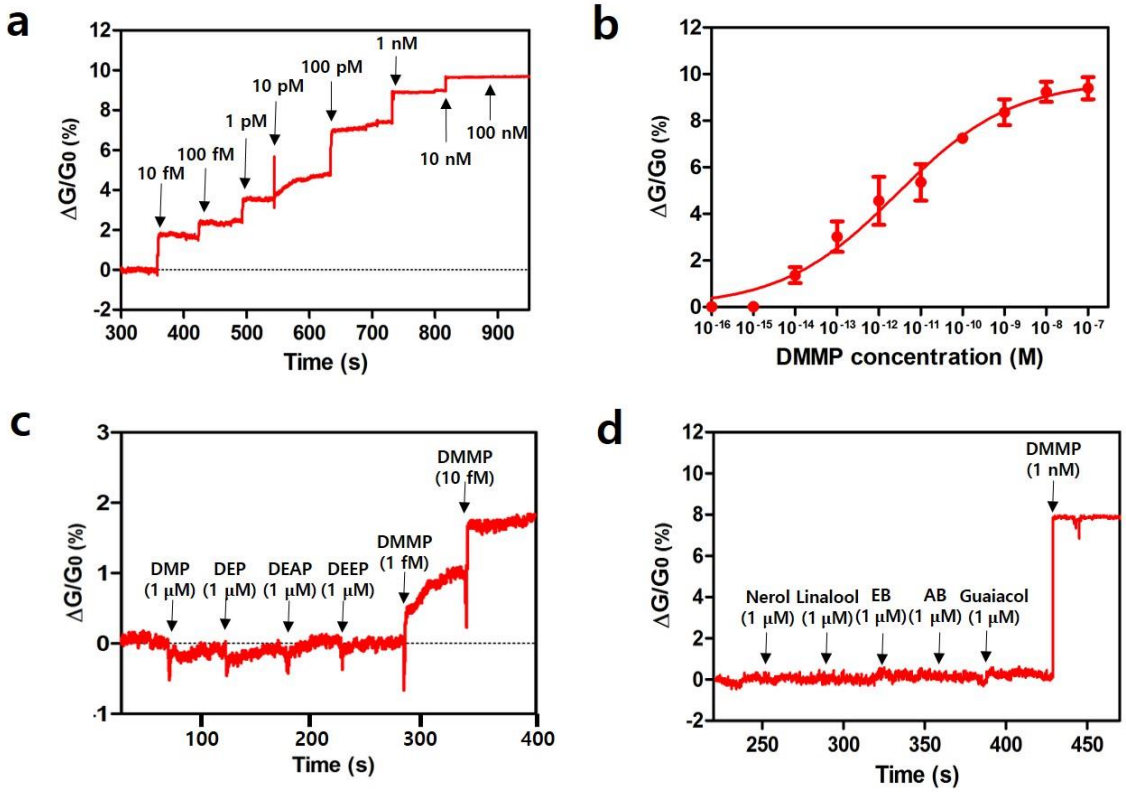
a
ΔG/G0 (%)
Time (s)
10 fM
100 fM
1 pM
10 pM
100 pM
1 nM
10 nM
100 nM
b
ΔG/G0 (%)
DMMP concentration (M)
c
ΔG/G0 (%)
Time (s)
DMP (1 μM)
DEP (1 μM)
DEAP (1 μM)
DEEP (1 μM)
DMMP (1 fM)
DMMP (10 fM)
d
ΔG/G0 (%)
Time (s)
Nerol (1 μM)
Linalool (1 μM)
EB (1 μM)
AB (1 μM)
Guaiacol (1 μM)
DMMP (1 nM)

Supporting Information

Olfactory receptor-based CNT-FET sensor for the detection of DMMP as a simulant of sarin

[a]School of Chemical and Biological Engineering, Institute of Chemical Processes, Seoul National University, Seoul 08826, Republic of Korea.

[b]Department of Biophysics and Chemical Biology, Seoul National University, Seoul 08826, Republic of Korea.

[c]Department of Physics and Astronomy and Institute of Applied Physics, Seoul National University, Seoul 08826, Republic of Korea

[†]These authors contributed equally to this work.

* Corresponding author at: Department of Physics and Astronomy and Institute of Applied Physics, Seoul National University, Seoul 08826, Republic of Korea.

**Corresponding author at: School of Chemical and Biological Engineering, Seoul National University, Seoul 08826, Republic of Korea.

Tel: +82-2-880-8020; Fax: +82-2-875-9348;

E-mail: shong@phya.snu.ac.kr (S. Hong), thpark@snu.ac.kr (T. H. Park)

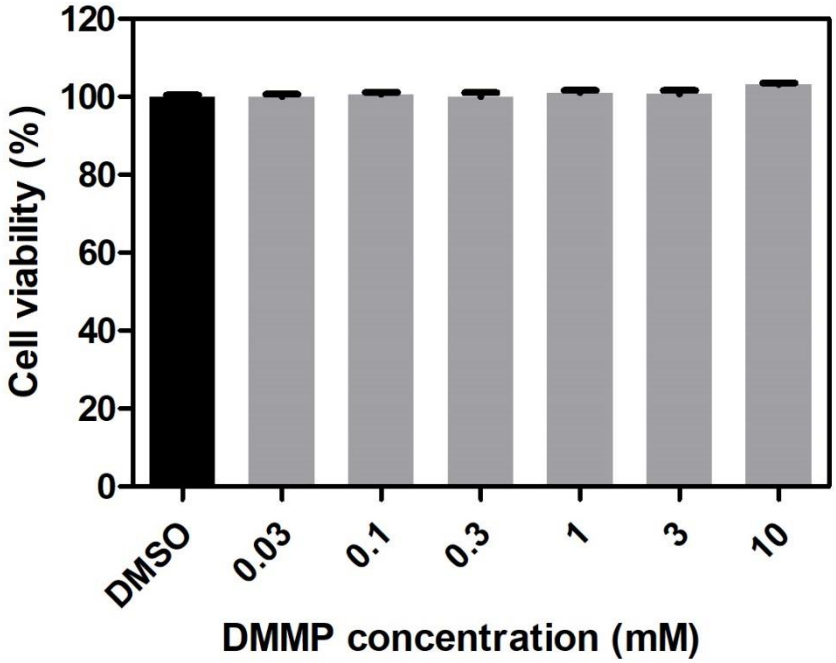

Figure S1. Cytotoxicity analysis of DMMP. Hana3A cells were treated with DMMPs in the range of concentrations (0.03 to 10) mM, and cell viability was compared with a control that was treated with DMSO.

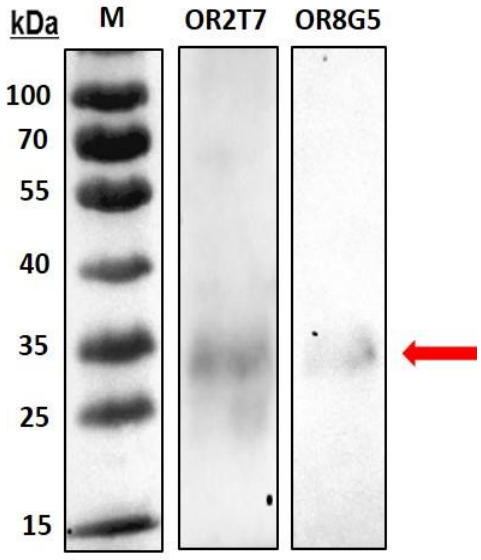

Figure S2. Western blot analysis of OR2T7 and OR8G5 expressed in Hana3A cells.

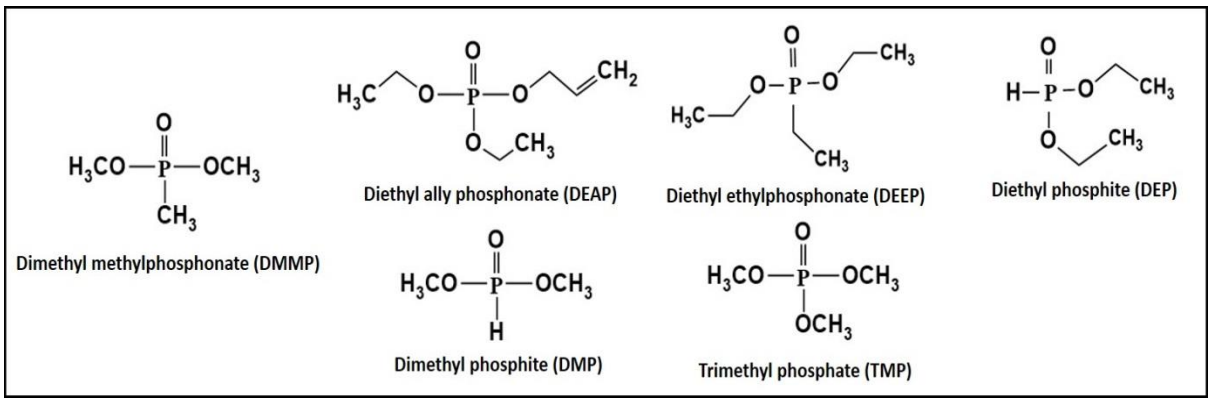

Figure S3. Odor molecules that are structurally similar to DMMP

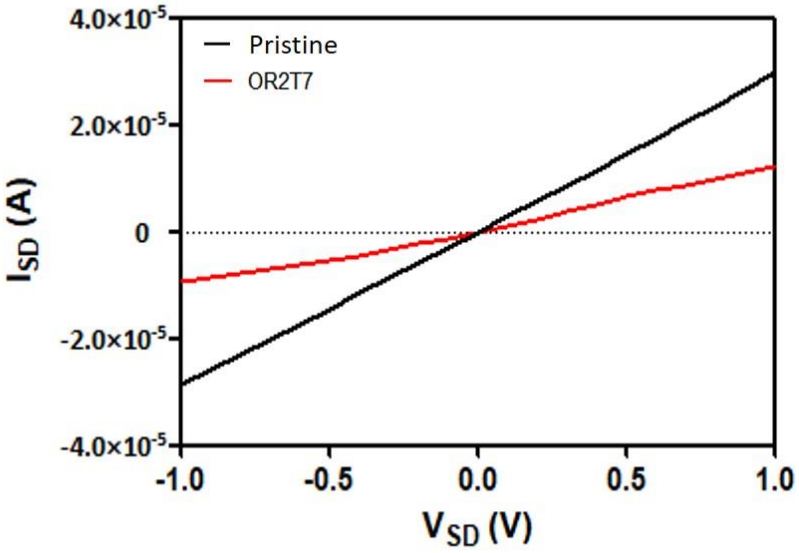

Figure S4. Current–voltage curves of the bare CNT channel (pristine), and CNT channel functionalized with OR2T7.

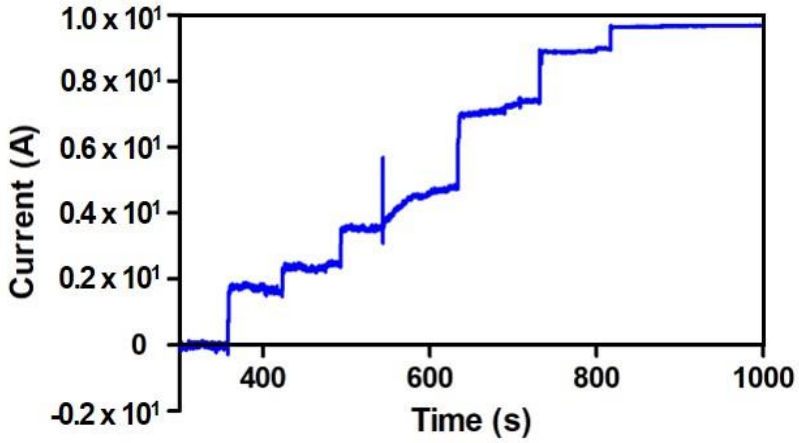

Figure S5. Real-time current changes of a hOR2T7 B-nose with various concentrations of DMMP